CALCULATION OF THERMODYNAMICAL, TRANSPORT AND STRUCTURAL PROPERTIES OF NEON IN LIQUID AND SUPERCRITICAL PHASES BY MOLECULAR DYNAMICS SIMULATIONS USING AN ACCURATE *ab initio* PAIR POTENTIAL

Muthusamy VENKATRAJ[a1], Markus G. MÜLLER[a2], Hanspeter HUBER[a3,*] and Robert J. GDANITZ[b,+]

[a] *Departement Chemie, Universität Basel, Klingelbergstrasse 80, CH-4056, Basel, Switzerland; e-mail: [1] m.venkatraj@unibas.ch, [2] markus.mueller@unibas.ch, [3] hanspeter.huber@unibas.ch*

[b] *Department of Chemistry, University of Utah, 315 S. 1400 E, Rm 2020, Salt Lake City, UT 84112, U.S.A.; e-mail: gdanitz@hec.utah.edu*

Received August 20, 2002
Accepted November 22, 2002

Dedicated to Professors Petr Čársky, Ivan Hubač and Miroslav Urban on the occasion of their 60th birthdays.

An analytical potential energy curve (NE3) is constructed from points obtained by accurate *ab initio* calculations. The quality of the pair potential is established by a comparison of calculated and experimental second virial coefficients as a function of temperature. Molecular dynamics equilibrium simulations are performed with the NE3 potential for pressures between 20 and 1000 MPa and temperatures between 100 and 600 K in the supercritical phase and for one point in the liquid phase of neon. The properties are compared with those obtained from experiment. It is found that the accurate pair potential has a large effect on pressure, energies and enthalpies and a significant influence on other thermodynamic properties but little influence on transport and structural properties. In the supercritical phase the deviation between the calculated quantum-corrected and experimental pressure values is always less than 2%.

Keywords: Molecular dynamics simulations; Neon; Thermodynamics; *Ab initio* pair potential; Computational chemistry.

Application of molecular dynamics and Monte Carlo simulations in predicting the fluid properties with model and empirical potentials was very

+ On leave from: Institute for Physical and Theoretical Chemistry, Technical University Braunschweig, Hans-Sommer-Str. 10, D-38106 Braunschweig, Germany.

popular in the past few decades. Use of *ab initio* potentials in simulations started only about two decades ago by Clementi and co-workers[1,2], to calculate everything from pure *ab initio* (global MD simulations). They have applied a complete *ab initio* potential for water in simulations[3–6] and calculated values for the evaporization energy, the diffusion coefficient, the dielectric relaxation time and structural properties. We have previously performed global MD simulations of neon with two pair potentials (NE1 and NE2, obtained from quantum chemical calculations of different quality) and calculated bulk properties of one-phase systems of neon[7–14]. The importance of quantum effects using a perturbational approach (NE2-WK) for the calculation of pair distribution function[15] and also the importance of three-body effects of liquid neon by combining the non-pair additive part of the three-body potential with two different pair potentials (NE1/TBI and NE2/TBI) was also studied by our group[16,17]. In addition, we have investigated the vapour-liquid phase coexistence of neon using Gibbs ensemble simulations by applying NE1 and NE2 pair potentials and also the pair potentials with an *ab initio* three-body potential[18]. The vapour-liquid phase coexistence of neon was also reported by Leonhard and Deiters[19]. They have applied an empirical Axilrod–Teller (AT) term with an *ab initio* pair potential instead of an *ab initio* three-body potential.

The goal of the present work is to apply the very recently calculated, highly accurate pair potential[20] (NE3) in molecular dynamics simulations and investigate the influence of the pair potential on different properties such as the internal energy U and the enthalpy H, the molar heat capacities $C_{V,\mathrm{m}}$ and $C_{P,\mathrm{m}}$, the speed of sound c, the adiabatic and isothermal compressibilities β_S and β_T, the thermal pressure coefficient γ_V and the differential Joule–Thompson coefficient μ, the self-diffusion coefficient D, the thermal conductivity λ and the shear viscosity η and the pair distribution function g.

METHOD AND CALCULATIONS

When constructing an analytical potential energy curve from *ab initio* points an additional point is included at a long distance of 100 nm (1890 a_0) with an energy of $0 \pm 0.38 \times 10^{-7}\ \mu E_\mathrm{h}$ to enforce convergence. The new potential (NE3) is applied in molecular dynamics simulations in a constant-NVE ensemble. The Verlet leap frog algorithm for a cubic box with periodic boundary conditions and the minimum image convention is used throughout. Long-range corrections are applied with a shifted potential for pressure and potential energy. Verlet neighbor lists are used. The simulations are started

from a face-centered-cubic (fcc) lattice with Gaussian distributed velocities scaled to correspond to the desired temperatures. Tests indicating when the equilibrium is reached were built into the program. In the beginning, the time step is increased for faster melting until the order parameter falls short of a given limit. Then the simulation is continued automatically with the normal time step until the temperature is constant and equal to the desired value. During this procedure, the temperature is rescaled every few time steps. Starting from a fcc state, it usually takes about 800 steps to reach the equilibrium. The equilibrium simulations for thermodynamic, transport and structural properties are carried out in eight, sixteen and four batches of 33 600 steps, respectively. The results of the single batches are used to estimate the standard error of the different properties.

All the simulations to calculate thermodynamic and transport properties are performed roughly at a given pressure and temperature, by taking the corresponding density from experiment and adjusting the energy in the equilibration phase of the simulation to yield a certain temperature. The densities are taken from Rabinovich *et al.*[21] and for pressures greater than 100 MPa from Le Neindre *et al.*[22] In the case of structural properties, the densities and temperatures are taken from Bellissent-Funel *et al.*[23] (at temperatures of 26.1, 36.4 and 42.2 K, and number densities of 60 459, 50 548 and 41 132 mol m^{-3}, respectively).

The following parameters are used for the final runs: 500 particles, time step length Δt 10 fs, cut-off radius 2.5 σ (σ = 276.6 pm is taken as the distance where the potential energy is zero) and list radius 2.9 σ. The parameters were tested to give no significant contribution to the errors of the results.

The thermodynamical properties are calculated using the equations as described in the refs[24,25]. The transport properties are obtained from the Green–Kubo integrals (for details, see refs[8–10]). Because of the fact that the simulated temperatures differ from the experimental temperatures by up to about 1%, the simulations are carried out at two different temperatures to enable the interpolation of the results to the experimental temperatures as given in Tables III–VII.

RESULTS AND DISCUSSION

Ab initio Potential

The *ab initio* points to construct our potential, referred to as NE3, were taken from the very recent work of Gdanitz[20]. The points were obtained

from the most elaborate *ab initio* potential of Ne_2 available from literature[26] by careful correction of the neglect of core-core and core-valence correlation, basis set incompleteness, missing contributions in CCSD(T) and relativistic effects.

In order to apply the highly accurate potential in simulations of many condensed phase properties of neon, we have constructed an analytical potential energy curve by fitting the *ab initio* points in Table I to the following analytical seven-parameter equation. The points were weighted according to their errors.

The seven-parameter potential has the form

$$E / E_h = \frac{a_1 e^{-a_2 x}}{1 + a_3 x + a_4 x^2} \left[1 - D_1(x)\right] - \left[\frac{a_5}{x^{10}} + \frac{a_6}{x^8} + \frac{a_7}{x^6}\right] D_2(x), \qquad (1)$$

where $x = r/a_0$, with r being the distance in atomic units and the damping functions D_1 and D_2, defined as $D_1 = \frac{1}{1 + e^{-10\frac{x-1.8897}{x}}}$ and $D_2 = \frac{1}{1 + e^{-10\frac{x-5.8582}{x}}}$, make the first part of Eq. (*1*) dominate at short distances and the second part at long distances. 10, 1.8897 (corresponding to 0.1 nm) and 5.8582 (corresponding to 0.31 nm) are arbitrarily chosen parameters, whereas the values of the fit parameters are

TABLE I
Interaction energies

Distance r/a_0	Energy[a] $E/\mu E_h$	Fitted energy μE_h	Distance r/a_0	Energy[a] $E/\mu E_h$	Fitted energy μE_h
4.25188	3412.02 ± 32	3412.11	6.14161	–122.02 ± 0.79	–122.51
4.72432	736.69 ± 10	736.56	6.61404	–91.31 ± 0.40	–91.37
5.19675	20.76 ± 3.2	20.69	7.08647	–63.39 ± 0.15	–63.02
5.66918	–125.08 ± 1.4	–124.44	7.55891	–42.82 ± 0.01	–42.82
5.81091	–131.03 ± 1.1	–131.16	8.50377	–20.68 ± 0.07	–20.48
5.85815	–131.53 ± 1.1	–131.56	9.44863	–10.49 ± 0.05	–10.55
5.90539	–131.08 ± 0.95	–131.28			

[a] Ref.[20]

a_1 = 36.96716549, a_2 = 1.491623225, a_3 = –0.4473750622, a_4 = 0.05383035913, a_5 = 9001.554804, a_6 = –63.87421384, a_7 = 7.267507761

Figure 1 shows a comparison of the pair potential NE3 with our previous *ab initio* pair potential NE2 [12] and the empirical pure pair potential HFD-B by Aziz and Slaman[27,28]. The NE3 potential has a well depth of 131.5 ± 0.9 μE_h, which agrees with the experimentally estimated depth of the neon-neon potential of 130.6 ± 4.6 μE_h [29,30].

Second Virial Coefficient

The second virial coefficient, which is a pure pair property, was calculated according to the procedure described in ref.[31] Table II shows the values of second virial coefficients with first- and second-order quantum corrections from NE3 potential (B_{NE3}, $B_{NE3\text{-}1QC}$ and $B_{NE3\text{-}2QC}$) and also the values from HFD-B potential ($B_{HFD\text{-}B}$) and experiment (B_{expt})[32,33] for a temperature range from 44 to 550 K. In addition, $B_{NE3\text{-}2QC} - B_{expt}$, $B_{HFD\text{-}B} - B_{expt}$ and $B_{NE3\text{-}2QC} - B_{HFD\text{-}B}$ values are also reported in the same Table. The second-order quan-

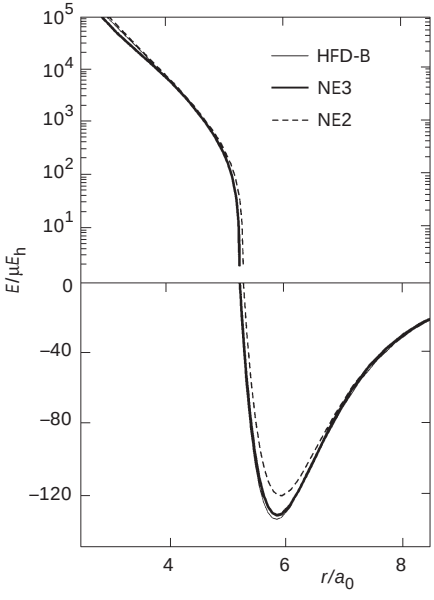

FIG. 1
Analytical potential energy curves of the neon dimer. Note the logarithmic scale for positive energies

TABLE II
Second virial coefficients

B, cm^3 mol^{-1}	T, K															
	44	50	60	70	80	100	125	150	200	250	300	350	400	450	500	550
B_{NE3}	–48.5	–37.8	–25.7	–17.7	–12.1	–4.7	0.8	4.3	8.2	10.3	11.6	12.4	13.0	13.3	13.6	13.8
$B_{NE3\text{-}1QC}$[a]	–45.6	–35.7	–24.3	–16.7	–11.3	–4.1	1.2	4.6	8.4	10.5	11.7	12.5	13.0	13.4	13.6	13.8
$B_{NE3\text{-}2QC}$[b]	–45.1	–35.3	–24.1	–16.6	–11.2	–4.1	1.2	4.6	8.4	10.5	11.7	12.5	13.0	13.4	13.6	13.8
$B_{HFD\text{-}B}$[a]	–47.9	–37.5	–25.8	–17.9	–12.3	–5.0	0.5	4.0	7.9	10.1	11.4	12.2	12.7	13.1	13.4	13.6
B_{expt}	–46.1[c]	–35.4[c]	–24.9[c]	–17.1[c]	–12.8[d]	–6.0[d]	–0.4[d]	3.2[d]	7.7[d]	10.0[d]	11.3[d]	12.1[d]	12.7[d]	13.1[d]	13.4[d]	13.7[d]
$B_{NE3\text{-}2QC}$[b]–B_{expt}	1.0	0.1	0.8	0.5	1.6	1.9	1.6	1.4	0.7	0.5	0.4	0.4	0.3	0.3	0.2	0.1
$B_{HFD\text{-}B}$[a]–B_{expt}	–1.8	–2.1	–0.9	–0.8	0.5	1.0	0.9	0.8	0.2	0.1	0.1	0.1	0.0	0.0	0.0	–0.1
$B_{NE3\text{-}2QC}$[b]–$B_{HFD\text{-}B}$[a]	2.8	2.2	1.7	1.3	1.1	0.9	0.7	0.6	0.5	0.4	0.3	0.3	0.3	0.3	0.2	0.2

[a] Including first-order quantum correction according to ref.[31] [b] Including second-order quantum correction according to ref.[31] [c] Ref.[32] [d] Ref.[33], the experimental uncertainty is ±1 cm^3 mol^{-1}.

tum-corrected and experimental values of the second virial coefficient as a function of temperature is shown in Fig. 2. The second-order quantum corrected values are in agreement with experimental values within two standard errors. The values $B_{\mathrm{NE3\text{-}2QC}} - B_{\mathrm{expt}}$ and $B_{\mathrm{HFD\text{-}B}} - B_{\mathrm{expt}}$ show that there is a jump between the two temperatures 70 and 80 K. The experimental values below and above this temperature stem from different experiments[32,33]. The values $B_{\mathrm{NE3\text{-}2QC}} - B_{\mathrm{HFD\text{-}B}}$ do not show such a jump. Therefore we assume that the values from ref.[33] get too low at low temperatures. The values $B_{\mathrm{NE3\text{-}2QC}}$ are in excellent agreement with experimental values, except at low temperature from ref.[33] Hence, we conclude that the values $B_{\mathrm{NE3\text{-}2QC}}$ calculated from the NE3 potential are probably most accurate.

Pressure

First quantum corrections of pressure[34,35] were calculated for all the state points and the quantum-corrected pressures (P_{QC}) are reported along with classic pressures (P_{CL}) in Tables III and IV. The pressure shows a negative deviation from experimental values with increase in pressure. We estimate a statistical standard error of about 0.02% for the pressures. In the supercritical phase the deviation between the calculated quantum-corrected and experimental pressure values is always less than 2%. An explanation for the deviation of the simulated pressure from the experimental one is the neglect of many-body interactions. Interestingly, the deviation has a different

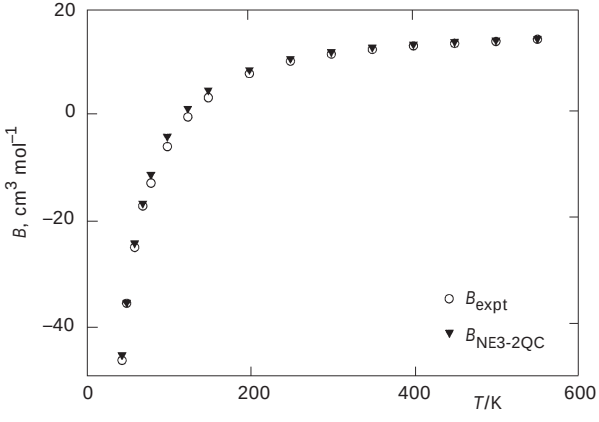

FIG. 2
Second virial coefficient of neon. A comparison between *ab initio* calculated and experimental values

TABLE III
Enthalpy H and energy U

T K	P_{expt} MPa	P_{NE3} MPa QC	P_{NE3} MPa CL	ρ mol m^{-3}	H_{NE3} J mol^{-1} (Δ, %)	H_{expt} [a] J mol^{-1}	U_{NE3} J mol^{-1} (Δ, %)	U_{expt} [b] J mol^{-1}
298	60	59.58	59.43	18436	6690(0.07)	6695	3458(0.06)	3460
	100	99.24	98.87	26472	7112(0.03)	7110	3363(0.3)	3372
	200	198.56	197.45	39693	8261(0.6)	8310	3259(0.7)	3281
	300	296.78	294.58	48118	9415(1.3)	9542	3247(0.7)	(3269)
	400	395.98	392.68	54411	10556(1.9)	10763	3278(0.3)	(3289)
	500	494.85	490.83	59367	11672(2.2)	11932	3337(0.4)	(3324)
	600	593.57	587.87	63480	12762(3.2)	13186	3412	
	700	691.86	684.96	66998	13824(3.8)	14369	3497	
400	60	60.05	59.98	14571	8957(0.6)	8900	4836(0.7)	4801
	100	100.03	99.84	21527	9426(0.6)	9370	4780(0.7)	4745

[a] Refs[36,37], values calculated by interpolation of experimental data. [b] Ref.[36], values calculated by interpolation and extrapolation (in parentheses) of experimental data.

sign than with our previous potentials (NE1 and NE2)[17]. The perfect agreement with experiment at low pressure and high temperature is a further indication that the pair potential is virtually exact.

Thermodynamical Properties

The calculated and experimental values[36,37] of the internal energy U and the enthalpy H for state points at room temperature and 400 K at pressures up to 700 MPa are reported in Table III. The deviation between the calculated and experimental internal energy values is less than 1%, *i.e.* chemical accuracy is attained for energies. In the case of the enthalpy values, the deviation is negligble at low pressures (60 and 100 MPa) and the deviation increases with increase in pressure (maximum 4%). The calculated and the experimental enthalpies as a function of the pressure are shown in Fig. 3. The reason for deviation of enthalpy values from experiment at high pressures is due to the three-body interactions. The calculated internal energy and enthalpy values have a statistical standard error of less than 0.5 J mol^{-1}.

The calculated and the available experimental data[21,36,38,39] for the molar heat capacities $C_{V,\mathrm{m}}$ and $C_{P,\mathrm{m}}$ and speed of sound c are given in Table IV. The points cover a wide range of the supercritical state between temperatures of 100 to 600 K and pressures of 20 to 1000 MPa. In addition, a point at 28 K is given to show the influence of quantum effects and many-body interactions. An excellent agreement is obtained while comparing the cal-

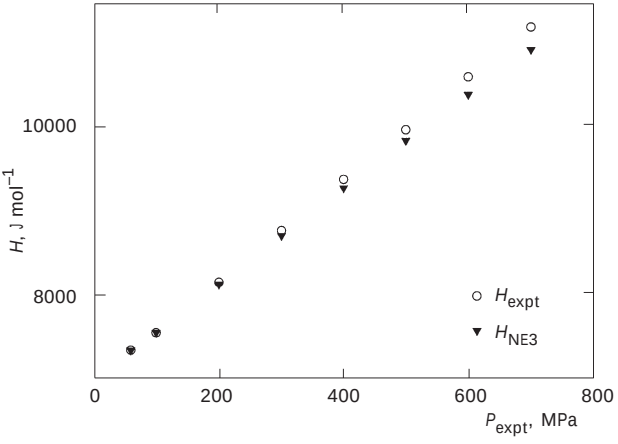

FIG. 3
Pressure dependence of the enthalpy H at room temperature. A comparison between *ab initio* calculated and experimental values

TABLE IV
Molar heat capacities and speed of sound[a]

T K	P_{expt} MPa	P_{NE3} MPa QC	P_{NE3} MPa CL	V_m 10^{-6} $m^3 mol^{-1}$	$C_{V,m}$ J mol^{-1} K^{-1}		$C_{P,m}$ J mol^{-1} K^{-1}		C_P/C_V		c m s^{-1}	
					NE3	expt	NE3	expt	NE3	expt	NE3	expt
298	60	59.58	59.43	54.24	13.2	13.2	22.4	22.6	1.70		605	602
298	100	99.24	98.87	37.78	13.6	13.6	22.9	23.0	1.68	1.70	697	693
298	200	198.56	197.45	25.19	14.5	14.5	23.5	23.6	1.62	1.63	890	891
298	300	296.78	294.58	20.78	15.2	15.2	24.0	24.0	1.58	1.58	1041	1053
298	400	395.98	392.68	18.38	15.8		23.9		1.51	1.53	1174	1177
298	500	494.85	490.83	16.84	16.4		24.5		1.49	1.49	1282	1289
298	600	593.57	587.87	15.76	16.9		24.9		1.47	1.46	1381	1389
298	700	691.86	684.96	14.93	17.4		25.4		1.46	1.44	1468	1479
298	800	790.51	782.38	14.27	17.9		25.8		1.44	1.42	1548	1561
298	900	887.19	877.79	13.74	18.1		25.4		1.40	1.40	1624	1636
298	1000	989.33	978.58	13.27	18.5		25.9		1.40	1.38	1695	1706
100	20	19.89	19.55	44.88	13.8		29.8	30.0	2.16		358	
100	40	39.51	38.22	28.68	14.6		30.4	30.0	2.08		480	
100	60	58.94	56.57	23.79	15.2		30.2	29.2	1.99		575	
100	80	78.68	75.04	21.29	15.8		28.9	28.9	1.83		662	
100	100	99.23	94.42	19.66	16.3		29.3	28.8	1.80		730	735
200	20	19.99	19.94	93.11	12.9		22.5	22.9	1.74		434	
200	40	39.93	39.75	52.61	13.3		23.5	24.0	1.77		500	
200	60	59.83	59.45	39.35	13.6		24.3	24.5	1.79		562	
200	80	79.74	79.10	32.79	13.9		24.5	24.8	1.76		622	
200	100	99.58	98.63	28.86	14.2		24.5	24.9	1.73		679	677
400	60	60.05	59.98	68.63	13.0	12.8	21.7	21.7	1.67		655	634
500	60	60.05	60.01	82.78	12.9		21.4	21.3	1.66		700	
600	60	60.00	59.97	96.82	12.8		21.1	21.1	1.65		746	
400	100	100.03	99.84	46.45	13.3	13.1	22.1	21.9	1.66		732	711
500	100	99.99	99.88	55.01	13.2		21.7	21.5	1.64		770	
600	100	100.03	99.95	63.51	13.1		21.7	21.2	1.66		805	
28[b]	20	21.10	–4.73	15.74	21.9	17.7	47.6	38.4	2.17	2.17	659	581

[a] Refs[21,36,38], experimental values. [b] Refs[21,39], experimental values for this temperature are from a slightly different density (16.95×10^{-6} m^3 mol^{-1}).

culated $C_{V,m}$ and $C_{P,m}$ and C_P/C_V values in the supercritical region with the available experimental values. For the calculated molar heat capacities $C_{V,m}$ and $C_{P,m}$ we estimate a statistical standard error of about 0.05 and 0.1 J mol^{-1} K^{-1}, respectively, and the statistical standard error estimated in the calculated C_P/C_V value is about 0.03. In the case of the liquid, the calculated $C_{V,m}$ and $C_{P,m}$ values are higher than the experimental values. The calculated C_P/C_V value agrees well with experiment. The reason for the large deviation of molar heat capacity values from experiment in the liquid region must be mainly due to quantum effects and to a minor extent to many-body interactions. The large influence of quantum effects at this temperature is seen for the pressure in the same Table. The molar heat $C_{V,m}$ for the liquid is also evaluated in an alternative way as the numerical derivative of the internal energy U with respect to temperature. The value 21.8 J mol^{-1} K^{-1} calculated in this way is in very good agreement with the simulated value 21.9 J mol^{-1} K^{-1} as reported in Table IV.

The calculated sound velocity is in quite good agreement with experiment. We estimate the statistical error of the calculated values to about 0.5 m s^{-1}. A comparison between the calculated values at room temperature up to 1000 MPa with experimental values is given in Fig. 4. The deviation between the calculated and the experimental speed of sound values at room temperature for pressures up to 1000 MPa, at 100 K/100 MPa and at 200 K/100 MPa is about 1% and the value for the remaining points is 3%.

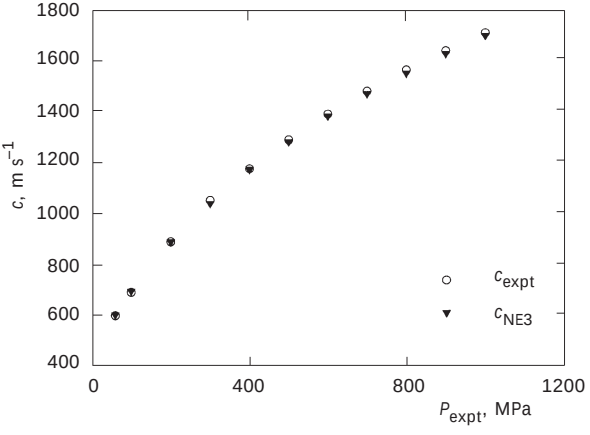

FIG. 4
Pressure dependence of the sound velocity c at room temperature. A comparison between *ab initio* calculated and experimental values

In the case of the liquid (28 K/20 MPa), the deviation increases to 13% which is mainly due to quantum and many-particle effects.

The calculated and the available experimental data[21,36,38,39] for other thermodynamic properties which are derivatives of the state function such as the adiabatic and the isothermal compressibilities β_S and β_T, the thermal pressure coefficient γ_V and the differential Joule–Thompson coefficient μ, are given in Table V. The statistical standard error of the calculated adiabatic compressibility β_S is about 0.01 GPa^{-1} and the calculated isothermal compressibility β_T 0.02 GPa^{-1}. Both compressibilities are at room temperature over the whole pressure range in excellent agreement with experiment. The calculated differential Joule–Thompson coefficient has a statistical standard error of about 0.025 K MPa^{-1}. The deviation between the calculated and experimental differential Joule–Thompson coefficient values at 298 K/60 MPa and at 400 K/60 MPa is about 10%. In the case of points at room temperature with pressure range from 100 to 300 MPa and at 400 K/100 MPa, the values are in good agreement (within the statistical error) with experiment.

Comparison of the calculated thermodynamical properties from the pair potential NE3 with the values obtained from our previous potentials NE1 [11] and NE2 [13] indicates that the pair potential NE3 has a large effect on pressure, energies and enthalpies and a significant influence on other thermodynamic properties. Thermodynamic derivatives are obtained very accurately. The reason for this is probably an error cancellation which might be seen, for example, when taking a numerical derivative of the internal energy with respect to temperature (difference of internal energy values of neighboring state points divided by difference of their temperatures).

Transport Properties

Transport properties for three selected points in the supercritical region are calculated and reported in Table VI. To decrease the statistical error for the time correlation functions which are used to obtain the the transport properties, 537,600 steps have been carried out for each of the three points in the supercritical region. The self-diffusion coefficient, obtained with a very small statistical error, is not known experimentally for the supercritical state and hence no comparison is possible. The calculated thermal conductivity and viscosity values are in good agreement with the experimental values[22,40,41] but the statsitical errors for these two properties are still large (maximum 6%).

TABLE V
Several thermodynamical properties[a]

T K	P_{expt} MPa	V_m 10^{-6} m^3 mol^{-1}	β_S, GPa^{-1}		β_T, GPa^{-1}		γ_V, MPa K^{-1}		μ, K (MPa)$^{-1}$	
			NE3	expt	NE3	expt	NE3	expt	NE3	expt
298	60	54.24	7.34		12.48		0.214		–0.498	–0.457
298	100	37.78	3.86	3.85	6.48	6.52	0.356		–0.516	–0.494
298	200	25.19	1.58	1.57	2.55	2.57	0.685		–0.514	–0.506
298	300	20.78	0.94	0.94	1.49	1.48	0.974		–0.489	–0.492
298	400	18.38	0.66	0.66	1.00	1.01	1.219		–0.488	
298	500	16.84	0.51	0.50	0.76	0.75	1.461		–0.460	
298	600	15.76	0.41	0.41	0.60	0.59	1.681		–0.441	
298	700	14.93	0.34	0.34	0.50	0.49	1.893		–0.422	
298	800	14.27	0.29	0.29	0.42	0.41	2.089		–0.407	
298	900	13.74	0.26	0.25	0.36	0.36	2.220		–0.411	
298	1000	13.27	0.23	0.23	0.32	0.31	2.415		–0.394	
100	20	44.88	17.38		37.45		0.308		0.231	
100	40	28.68	6.18		12.82		0.655		–0.151	
100	60	23.79	3.56		7.06		0.946		–0.261	
100	80	21.29	2.41		4.42		1.184		–0.350	
100	100	19.66	1.83		3.29		1.419		–0.357	
200	20	93.11	24.51		42.81		0.110		–0.245	
200	40	52.61	10.41		18.47		0.230		–0.337	
200	60	39.35	6.17		10.98		0.351		–0.371	
200	80	32.79	4.19		7.38		0.468		–0.414	
200	100	28.86	3.10		5.35		0.578		–0.451	
400	60	68.63	7.93		13.20		0.154		–0.584	–0.529
500	60	82.78	8.37		13.93		0.122		–0.585	
600	60	96.82	8.63		14.22		0.100		–0.668	
400	100	46.45	4.30		7.12		0.258		–0.558	–0.550
500	100	55.01	4.60		7.59		0.202		–0.592	
600	100	63.51	4.84		8.10		0.168		–0.541	
28[b]	20	15.74	1.81	2.52	3.94	5.49	3.87	2.83	–0.192	

[a] Refs[21,36,38], experimental values. [b] Ref.[39], experimental values for this temperature are from a slightly different density (16.95 × 10^{-6} m^3 mol^{-1}).

Structural Properties

For a discussion of the structural properties, we use the radial distribution function *g*. Table VII shows the position and height of the first maximum of the calculated and experimental[23] radial distribution functions of neon for three points in the liquid phase. The first maximum of the radial distribution function from classic potential NE3 overshoots the experimental value by 18, 14 and 9% at three temperatures 26.1, 36.4 and 42.2 K, respectively. As the many-body effects are negligble for liquid neon at low tem-

TABLE VI
Pressure dependence of transport properties in the supercritical state at 298 K

P_{expt} MPa	V_m 10^{-6} m^3 mol^{-1}	$10^{10}D$ m^2 s^{-1}	λ W m^{-1}K^{-1}		η μPa s	
		NE3	NE3	expt[a]	NE3	expt[b]
100	37.78	635.1±0.7	0.0817±0.0030	0.0785±0.0008	40.33±1.49	42.61±0.21
						42.91±0.43
500	16.84	205.5±0.4	0.1847±0.0120	0.1909±0.0019	89.98±5.53	97.11±0.49
1000	13.27	124.8±0.2	0.3317±0.0193	0.3112±0.0031	168.53±6.20	165.23±0.83

[a] Ref.[22], experimental values. [b] Refs[40,41], interpolated from experimental values.

TABLE VII
Position and height of the first maximum of the radial distribution functions of neon

T, K	Method	*r*, pm	*g*
26.1	NE3	303	2.92
	NE3-WK	314	2.60
	expt[a]	310	2.47
36.4	NE3	305	2.45
	NE3-WK	311	2.30
	expt[a]	309	2.15
42.2	NE3	303	2.22
	NE3-WK	310	2.12
	expt[a]	310	2.04

[a] Ref.[23], experimental values.

peratures[15] the large difference between the calculated and the experimental radial distribution functions must be due to the quantum effects. The calculated *g* values from the Wigner–Kirkwood quantum effective potential (NE3-WK, details in ref.[15]) indicate that the quantum effects are not reproduced fully for all these points. There is no significant change in *g* values for the potential (NE3) compared to the values obtained from our previous potentials (NE1 and NE2). Hence we conclude that the quality of the pair potential has little influence on structural properties.

CONCLUSIONS

From thermodynamical, transport and structural properties, calculated for neon over a wide range of pressures (up to 1000 MPa) and temperatures (up to 600 K) with the new, highly accurate pair potential (NE3), we conclude that:

– At pressures up to about 200 MPa and temperatures above 200 K, these properties can be obtained *ab initio* within chemical accuracy.

– The new NE3 potential is probably by far the most accurate potential that is available, in particular more accurate than any empirical pure pair potential.

– The new potential yields probably the most accurate second virial coefficients that are available.

– Even at the highest pressures, the deviation for the pressure from experiment is less than 2%, if first-order quantum corrections are included.

– It, however, turns out to be impossible to get high accuracy for liquid-phase points without inclusion of many-body and quantum effects.

Because of the high accuracy of the NE3 potential used in the present work, the accuracy that can be obtained in MD simulations is now given by the limited statistics for reasonably long runs in the case of the transport properties (diffusion, thermal conductivity and shear viscosity), and by the classic mechanics and pair-additivity approximation for all properties at low temperatures or extremely high pressures, for neon in particular any liquid-phase points.

LIST OF SYMBOLS

B	second virial coefficient, $cm^3\ mol^{-1}$
$C_{V,m}$	molar heat capacity at constant volume, $J\ mol^{-1}\ K^{-1}$
$C_{P,m}$	molar heat capacity at constant pressure, $J\ mol^{-1}\ K^{-1}$
c	speed of sound, $m\ s^{-1}$
D	self-diffusion coefficient, $m^2\ s^{-1}$

E	energy, μE_h
g	radial distribution function
H	enthalpy, J mol^{-1}
p	pressure, MPa
r	distance, a_0
T	temperature, K
Δt	time step length, fs
U	internal energy, J mol^{-1}
β_s	adiabatic compressibility, GPa^{-1}
β_T	isothermal compressibility, GPa^{-1}
γ_v	thermal pressure coefficient, MPa K^{-1}
η	shear viscosity, μPa s
λ	thermal conductivity, W m^{-1} K^{-1}
μ	differential Joule–Thompson coefficient, K MPa^{-1}
ρ	density, mol m^{-3}
σ	distance where the potential energy is zero, pm

M. Venkatraj thanks ESKAS, Switzerland, for financial support in the form of a fellowship. H. Huber thanks Prof. H. Thomas, Basel, for a helpful discussion. This investigation is a part of the Project 2000-066530.01 of the Schweizerischer Nationalfonds zur Förderung der Wissenschaften. R. J. Gdanitz acknowledges German "Deutsche Forschungsgemeinschaft" (DFG) (GD1/6-1) for support of this work.

REFERENCES

1. Clementi E.: *Modern Techniques in Computational Chemistry MOTECC-90*. ESCOM, Leiden 1990.
2. Clementi E., Corongiu G., Bahattacharya D., Feuston B., Frye D., Preiskorn A., Rizzo A., Xue W.: *Chem. Rev. (Washington, D. C.)* **1991**, *91*, 679.
3. Matsuoka O., Clementi E., Yoshimine M.: *J. Chem. Phys.* **1976**, *64*, 1351.
4. Niesar U., Corongiu G., Huang M.-J., Dupuis M., Clementi E.: *Int. J. Quantum Chem. Quantum Chem. Symp.* **1989**, *23*, 421.
5. Niesar U., Corongiu G., Clementi E., Kneller G. R., Bhattacharya D. K.: *J. Phys. Chem.* **1990**, *94*, 7949.
6. Corongiu G.: *Int. J. Quantum Chem.* **1992**, *42*, 1209.
7. Eggenberger R., Gerber S., Huber H., Searles D.: *Chem. Phys.* **1991**, *156*, 395.
8. Eggenberger R., Gerber S., Huber H., Searles D., Welker M.: *Mol. Phys.* **1992**, *76*, 1213.
9. Eggenberger R., Gerber S., Huber H., Searles D., Welker M.: *Chem. Phys.* **1992**, *164*, 321.
10. Eggenberger R., Gerber S., Huber H., Searles D., Welker M.: *J. Phys. Chem.* **1993**, *97*, 1980.
11. Eggenberger R., Gerber S., Huber H., Searles D., Welker M.: *J. Chem. Phys.* **1993**, *99*, 9163.
12. Eggenberger R., Gerber S., Huber H., Welker M.: *Mol. Phys.* **1994**, *82*, 689.
13. Eggenberger R., Huber H., Welker M.: *Chem. Phys.* **1994**, *187*, 317.
14. Huber H., Dyson A. J., Kirchner B.: *Chem. Soc. Rev.* **1999**, *28*, 121.
15. Ermakova E., Solca J., Huber H., Marx D.: *Chem. Phys. Lett.* **1995**, *246*, 204.

16. Ermakova E., Solca J., Steinebrunner G., Huber H.: *Chem. Eur. J.* **1998**, *4*, 377.
17. Kirchner B., Ermakova E., Solca J., Huber H.: *Chem. Eur. J.* **1998**, *4*, 383.
18. Vogt P. S., Liapine R., Kirchner B., Dyson A. J., Huber H., Marcelli G., Sadus R.: *Phys. Chem. Chem. Phys.* **2001**, *3*, 1297.
19. Leonhard K., Deiters U. K.: *Mol. Phys.* **2000**, *98*, 1603.
20. Gdanitz R. J.: *Chem. Phys. Lett.* **2001**, *348*, 67.
21. Rabinovich V. A.,Vasserman A. A., Nedostup V. I., Veksler L. S.: *Thermophysical Properties of Neon, Argon, Krypton, and Xenon*. Hemisphere Publishing Corporation, Washington 1988.
22. Le Neindre B., Garrabos Y., Tufeu R.: *Physica A (Amsterdam)* **1989**, *156*, 512.
23. Bellissent-Funel M. C., Buontempo U., Filabozzi A., Petrillo C., Ricci F. P.: *Phys. Rev. B: Condens. Matter* **1992**, *45*, 4605.
24. Allen M. P., Tildesley D. J.: *Computer Simulation of Liquids*. Clarendon Press, Oxford 1987.
25. Thompson S. M.: *CCP5 Program Library 1980*.
26. Cybulski S. M., Toczylowski R. R.: *J. Chem. Phys.* **1999**, *111*, 10520.
27. Aziz R. A., Slaman M. J.: *Chem. Phys.* **1989**, *130*, 187.
28. Slaman M. J., Aziz R. A.: *Chem. Eng. Commun.* **1991**, *104*, 139.
29. Tanaka Y., Yoshino K.: *J. Chem. Phys.* **1972**, *57*, 2964.
30. Le Roy R. J., Klein M. L., McGee I. J.: *Mol. Phys.* **1974**, *28*, 587.
31. Hirschfelder J. O., Curtiss C. F., Bird R. B.: *Molecular Theory of Gases and Liquids*. Wiley, New York 1954.
32. Gibbons R. M.: *Cryogenics* **1969**, *9*, 251.
33. Dymond J. H., Smith E. B.: *The Virial Coefficients of Gases, A Critical Compilation*. Clarendon Press, Oxford 1969.
34. Ree F. H.: *J. Phys. Chem.* **1983**, *87*, 2846.
35. Barker J. A., Fisher R. A., Watts R. O.: *Mol. Phys.* **1971**, *21*, 657.
36. Michels A., Wassenaar T., Wolkers G. J.: *Physica* **1965**, *31*, 237.
37. Maslennikova V. Y., Egorov A. N., Tsiklis D. S.: *Sov. Phys. Dokl.* **1976**, *21*, 440.
38. Kortbeek P. J., Biswas S. N., Schouten J. A.: *Int. J. Thermophys.* **1988**, *9*, 803.
39. Naugle D. G.: *J. Chem. Phys.* **1972**, *56*, 5730.
40. Vermesse J., Vidal D.: *Acad. Sci., Ser. II* **1975**, *280*, 749.
41. Trappeniers N. J., Botzen A., Van den Berg H. R., Van Oosten J.: *Physica* **1964**, *30*, 985.